

Selective source reduction to identify masked sources using time reversal acoustics

M Scalerandi¹, A S Gliozzi¹, Brian E Anderson², M Griffa², Paul A Johnson² and T J Ulrich²

¹ CNISM, Physics Department, Politecnico di Torino, C.so Duca degli Abruzzi 24, 10129 Torino, Italy

² Los Alamos National Laboratory, Geophysics Group, Los Alamos, NM 87544, USA

E-mail: marco.scalerandi@infm.polito.it

Received 6 February 2008, in final form 20 May 2008

Published 9 July 2008

Online at stacks.iop.org/JPhysD/41/155504

Abstract

The presence of strong sources of elastic waves often makes it impossible to localize weaker ones, which are sometimes the most meaningful, e.g. in the characterization of complexity of active Earth faults or of microdamage in a composite structural material. To address this problem, a selective source reduction method is proposed here which, applied in conjunction with time reversal acoustics (TRA), provides the means to selectively reduce the contribution of strong sources allowing full illumination of the weak ones. The method is complementary to other methods based on TRA which aim at the selective illumination of scatterers in the propagation medium. In this paper, a description of the method is given along with presentation of a few numerical results to demonstrate its usefulness for localization of sources. Validation and some experimental results are also presented.

(Some figures in this article are in colour only in the electronic version)

1. Introduction

Earthquake source characterization [1], 3D localization of defects embedded in solid specimens [2] and imaging of structures inside biological tissues [3] are just a few important examples of research themes sharing a common issue: the localization and characterization of sources of elastic waves (primary or secondary, such as scatterers), in different frequency bands, ranging from infrasound to ultrasound.

Among the various methods developed for such purposes, time reversal acoustics (TRA) [4–7] has provided very promising techniques, due to the basic properties of time reversal (TR) (elastic) wave propagation and to its robustness and ease of implementation. TR refers to a process in which a propagating wave field is reversed in time and irradiated back towards the source from which it was generated [4], as discussed in section 2. Scatterers and nonlinear defects in a solid medium can be considered as secondary sources. Various TRA techniques have been developed for imaging and localization (illumination) of scatterers [8–14].

Nevertheless, when the material specimen or medium under investigation contains multiple sources located in

different positions, several issues arise which may cause failure of the illumination process. First of all, the spatial width of the point spread function, evaluated at the source location, and the side lobes generated by the discrete nature of the imaging system (array of sensors) may make the distinction difficult between separate sources, especially when they are closely located or when they are, for example, scatterers with very different strengths. There could also be close spatial and/or temporal relationships among the different sources. In the specific case of scatterers, multiple scattering could occur, giving rise to complicated patterns of signals which make the desired localization and characterization very challenging. Difficulties emerge particularly in the resolution of closely located sources or in imaging of weak scatterers in the presence of much stronger ones.

The second case is especially relevant, since the presence of stronger sources generally makes it impossible to localize smaller, but often more meaningful, ones. This is the case in earthquake source mechanics, where usually the originating event is spatially and temporally complex. Further, multiple sources are present in materials containing distributions of microcracks or localized macrocracks evolving in time. In fact,

when a specimen containing these types of defects is insonified, nonlinear interaction processes occur between the defects and the probing elastic waves. The nonlinearity adds new frequency content to the propagating waves (higher order harmonics, sum and difference frequencies). The microcracks, as nonlinear scatterers, could be described as sources of new temporal frequencies. A technique based on TRA and called time reversal nonlinear elastic wave spectroscopy (TR-NEWS) [12, 15, 16] has been developed for exploiting the nonlinearly added frequency content and retrofocusing elastic energy only on the nonlinear scatterers.

As shown by the example of nonlinear scatterers mentioned above, the definition of acoustic sources includes different features. A first class is primary sources which generate an elastic wave(s) (not as a response to an incoming wave). These include transducers, sources of acoustic emission events and earthquake sources. On the other hand, we classify secondary sources as those which generate an elastic wave in response to a given dynamic elastic excitation. This class is mostly made up of scatterers in the propagation medium. This distinction is, in our opinion, important in understanding the focus of our work and its novelty with respect to existing approaches. In fact, several TRA methods have been developed to address the issue of selective localization: the iterative time reversal mirror [17], the decomposition of the time reversal operator (DORT) [18, 19] and the time reversal acoustics multiple signal classification (TRA-MUSIC) imaging technique [20]. These methods address the issue of the selective localization of embedded targets, i.e. linear scatterers. However, the extension of their applicability to nonlinear scatterers, e.g. in order to exploit TR-NEWS [12, 15], is not straightforward because of the increase in the nonlinear frequency content at every iteration of the procedure. In contrast, we propose an approach for selective source reduction (SSR-TRA) which aims at reducing the focusing on dominant primary sources in order to illuminate other sources, smaller in amplitude and/or spatial extension, through successive cancellation of the dominant sources in the specimen. As such, it can be considered as complementary to other methods, as discussed in section 2.

The theoretical background of this new method, presented in section 4, is not limited by typical restrictive assumptions about the configuration of the system: indeed the same method can be applied to locate both isotropic and anisotropic, well resolved and not well resolved, point-like and extended targets. Also, the approach presented here does not require *a priori* knowledge about the sources to be detected, nor the repeatability of the emission event. Furthermore, it exploits the full temporal signals (i.e. direct propagation and coda) for the selection of sources. As a consequence of the use of signals including multiple reflections and scattering inside the specimen of investigation (the coda portion contains such information), few TR channels (at least one, as shown by the experimental results reported) are sufficient to implement this new method in practice. Note that, although they are aimed at different problems, this is one of the main advantages of the SSR-TRA method with respect to DORT or TRA-MUSIC techniques, which require at least as many channels as the

number of sources/scatterers. The experimental validation also shows that the SSR-TRA method is not limited to experimental configurations with the time reversal mirror (TRM) [5] and the specimen under investigation submerged in a water tank used as a coupling medium for the propagation of waves. In fact, the transducers can be directly bonded on the surface of the specimen itself, common in non-destructive evaluation (NDE) techniques exploiting ultrasound acoustic waves.

As it will be clarified later, SSR-TRA is based on the possibility of measuring signals in the location of the focal regions of the TRA procedure. From an experimental point of view a potential limitation can be due to the finite size of the transducers. When the size of the transducer is large with respect to the corresponding size of the focal spot (which usually occurs), the signal recovered includes additional contributions of the backpropagated wave field other than just the focused ones [21]. Nevertheless, experimental studies currently in progress indicate that the method still works for transducers of finite size.

A more critical issue is that the experimental procedure is applicable only to surface sources (to be reduced) since transducers must be placed at the location of the focal spot. Therefore, the surface must be accessible for transducer interrogation, which is not always the case for applications in NDE. Nevertheless, some cases in which sources are localized on the surface or just below (the method may still approximately work) have practical importance, such as for the reduction of the nonlinear signal generated by a non-perfect transducer when imaging nonlinear scatterers using TR-NEWS [12–15]. Nevertheless, when the source to be reduced is embedded, SSR-TRA requires an analysis based on simulations of the wave propagation with the use of reliable materials models (with longitudinal and shear velocities of the specimen known with good accuracy) to substitute the full experimental procedure. In this case, part of the advantages of the SSR-TRA method over other advanced variants of the TR technique are lost, though other methods do not provide the means of going beyond the masking problem with close proximity sources.

In this paper, we consider a typical test experiment, described in section 3, and discuss the SSR-TRA method and theoretical background (section 4). Its efficiency is shown by means of modelling results obtained from simulations performed using a full 3D local interaction simulation approach (LISA) [22, 23]. In section 5 improvements on the method and a brief discussion of its potential are given. Validation through experimental results is presented in section 6. In the present contribution, we deal with ideal surface point-like sources (i.e. with size much smaller than the size of the focal spot, which is typically of the order of half the central wavelength), realized in the experiment using a laser vibrometer.

2. State of the art

2.1. TRA experiments

Standard TRA experiments consist of two stages. First, a forward propagation stage, during which an array of

transducers, called TRM [5], records a set of signals generated by elastic wave propagation throughout the medium, carrying information about it. These forward wave fields may be created by primary sources (transducers attached to the surface of a laboratory specimen or embedded acoustic emission sources or earthquake sources) or may be the result of backscattering processes after the medium have been insonified by the TRM itself or by other primary sources. This first stage is followed by a TR backward propagation stage, during which the same signals are processed, reversed in time and re-emitted by the same transducers, now acting as sources. Consequently, wave fields are generated and propagate throughout the medium following approximately the same ray paths of the forward propagation but with opposite directions. These wave fields focus back onto regions containing sources (primary or secondary) [6, 7]. Multiple scattering, instead of limiting the retrofocusing, as it happens with many other imaging techniques, actually enhances the efficiency of the retrofocusing [5, 24] and the use of the full length of the signal corresponds to an effective increase in the aperture of the TRM.

The robustness of TRA in solids [25–28] and nonlinear elastic media [25, 29, 30] has indeed triggered the development of TRA techniques for imaging and localizing scatterers [8, 9], including the case of defects in damaged solid specimens [10, 11].

2.2. Selective localization of multiple targets

Many different TRA techniques have been developed and successfully implemented for addressing the problem of the selective localization of embedded targets. Most of them are aimed specifically at the problem of selectively localizing linear scatterers. Among them, the iterative time reversal mirror [5] is based on the iteration of the typical protocol of a reflection-mode TRA experiment: a TRM illuminates a medium containing several targets, with varying degrees of reflectivity, at different locations. Each signal is reversed in time and rebroadcast back by the same array. The procedure is iterated many times, with the resulting retrofocusing on the strongest scatterer after a few iterations [5].

Using frequency domain/matrix formalism, the convergence of the iterative TR procedure has been demonstrated theoretically and has led to another method for selective retrofocusing. This method has been called DORT, from the French acronym for the decomposition of the time reversal operator [18, 19]. DORT is based on the correspondence between each target/scatterer and the singular values of the inter-element frequency domain impulse response matrix of the system TRM/medium. DORT has been tested in numerous experiments [31] and applied to NDE purposes with solid specimens submerged in water containing well resolved (i.e. in the absence of multiple scattering) point-like [32] and/or finite size scatterers [33]. The basic theory of DORT relies on the assumption of a finite number of well resolved scatterers. Its generalization to the case of media containing poorly resolved targets has been performed using a multiple signal classification (MUSIC) scheme [34]. This scheme exploits the properties of orthogonality of the signal vector space, associated with

non-null singular values, and the noise space, which is associated with the remaining null singular values. It is possible to define a scalar field, function of space, which has local maxima at the positions of the scatterers, with maximum values proportional to the strength of the scatterers themselves [20]. The theory of the TRA-MUSIC selective localization technique has been also formulated considering a more general setup of multiple input/multiple output (MIMO) array of transducers, i.e. with forward propagation emitting transducers separate from the receiving/TR ones, in order to consider transmit-mode experiments [35].

Both DORT and TRA-MUSIC methods rely on the use of arrays of transducers containing several elements, at least as many as the number of embedded targets/scatterers. In general, this number is one of the unknown variables of the NDE problem. Furthermore, to our knowledge, DORT and TRA-MUSIC have been applied only to the selection of linear scatterers in the propagation medium and their extension to the detection of primary sources or elastic nonlinear scatterers has not yet been developed.

Multiple scattering may be caused by multiple reflections at the boundaries of a bounded medium. Some techniques based on an extended version of the DORT method have been developed by Song *et al* for the selective localization of scatterers in the presence of reverberation from the boundaries [36–38]. These techniques are aimed at the suppression of the reverberation from the boundaries of a shallow water ocean waveguide, at different ranges. However, they also rely on the use of a significant number of TRM elements. They inject elastic energy into the water column and, avoiding focusing on selected regions of the boundaries, provide a greater echo-to-reverberation enhancement. However, the image of the targets of interest can be obtained only through recovering their simple echoes. In the presence of closely spaced targets or with targets having different reflectivities there still remains the problem of their selective location. The iterative TR procedure can be implemented, starting from these echo signals, but it requires a very long and complicated procedure before obtaining the final image of the scatterers.

Another technique has been proposed in order to enhance the contrast between the parts of the wave fields due to the scattering at poor reflective targets and the ones due to strong multiple scattering induced by background clutter [39]. This technique, tested in the context of radar imaging, i.e. using electromagnetic waves, is aimed at nulling the backscattering contributions from the clutter and relies on a similar hypothesis as the DORT-based techniques: the number of strong clutter regions embedded in the propagation environment must be less or equal to the number of receiving channels.

A revised version of the iterative TR procedure has been proposed by Montaldo *et al* for addressing the problem of selective retrofocusing on distinct scatterers, avoiding the limitation of only focusing on the strongest one [40]. This method requires two additional steps in the traditional Iterative TR procedure: a correction of the retrieved signals at the TRM after the backscattering (in order to compensate for their broadening in time due to the transducers' transfer function), and a cancellation step to remove the contribution of the

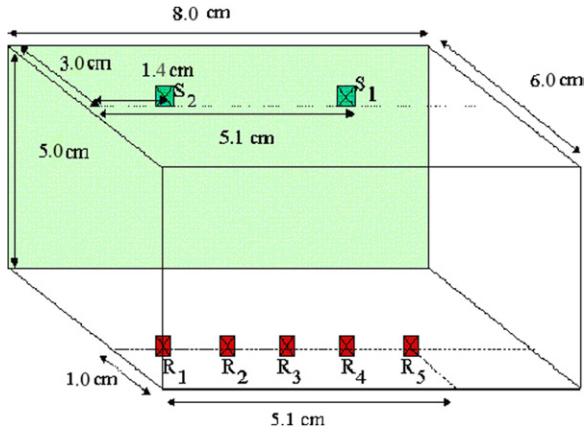


Figure 1. Setup of the virtual experiments. Two sources S_1 and S_2 are located on the upper surface of a specimen and five equally spaced receivers are located on the bottom surface.

strongest scatterer. Iteratively, this last step can lead to the successive removal of the contributions of the different scatterers to the backscattered wave fields until only the ones from the weakest scatterer remain. This method also relies on the use of a large number of TRM transducers and is based in part upon a modelling hypothesis for the description of the echo signals for the different iterations.

3. Setup of the simulations

3.1. Description of the simulation

To perform our analysis, we consider a very simple simulation. The specimen physical characteristics correspond to that of a metal block of dimensions $8 \times 6 \times 5 \text{ cm}^3$, as shown in figure 1. The volumetric mass density is $\rho = 2770 \text{ kg m}^{-3}$ and the longitudinal and shear wave velocities are $v_L = 5098 \text{ m s}^{-1}$ and $v_S = 3064 \text{ m s}^{-1}$, respectively. Attenuation is neglected in the simulations.

The specimen has two point-like sources, S_1 and S_2 , located on the upper surface at $(x_j, y_j, z_j) = (5.1, 3.0, 0.0)$ and $(1.4, 3.0, 0.0) \text{ cm}$, respectively. An array of five equally spaced receivers R_k ($k = 1-5$) is arranged on the lower surface (see figure 1). The five receivers are located at the positions $(x_k, y_k, z_k) = (1.1, 5.0, 5.0)$, $(2.1, 5.0, 5.0)$, $(3.1, 5.0, 5.0)$, $(4.1, 5.0, 5.0)$ and $(5.1, 5.0, 5.0) \text{ cm}$. The receivers/sources act as sources/receivers when the TR back propagation stage is considered. Their arrangement has been chosen to avoid any possible symmetry in the configuration used.

The sources simultaneously inject an identical Gaussian modulated sine pulse signal (amplitudes vary),

$$u_{1,2}(t) = A_{1,2} \exp(-(t - t_0)^2/2\sigma^2) \sin(\omega t) \quad (1)$$

with angular frequency $\omega = 1.26 \text{ Mrad s}^{-1}$ and $t_0 = 6\pi/\omega \text{ s}$; $\sigma = 4\pi/\omega \text{ s}$.

Simulations were performed using the LISA [22, 23] for a full 3D elastic description of the wave propagation. The code has been implemented for a parallel computer using MPI libraries and a C compiler. A discretization of the specimen with space and time steps of 0.1 mm and 10^{-8} s ,

respectively, has proven to guarantee stability and convergence of the numerical solution. Details about the method and its validation are given elsewhere [22, 23] and not reported here for brevity.

3.2. The TRA simulation

We have conducted a simple TR simulation with two sources of amplitudes, $A_1 = 5A_2$. For our purposes, the relevant quantity is the amplitude ratio, so A_1 and A_2 can be expressed in arbitrary units. The implementation protocol is as follows:

- inject simultaneously the source signals $u_{1,2}(t)$ from the two sources (see equation (1));
- receive a signal $v_k(t)$ at each receiver and time reverse it within a proper time window of length Δ , starting from time t_0 ; let us call the time reversed signal $w_k(t) = v_k(t_0 + \Delta - t)$;
- rebroadcast simultaneously the signals $w_k(t)$ from the original receiver locations.

Note that the signals considered are, in general, the components of vector wave fields evaluated at the spatial positions of the transducers. In this regard, we consider, unless otherwise specified, the injected signals $u_j(t)$ in the form of in-plane (on the upper x - y surface) displacements, while the signals $v_k(t)$ recorded at receivers are out-of-plane (in the z -direction) components of the displacements. Tests have been performed to verify that the success of the SSR-TRA method is independent of the choice of the components of the signals.

The TR back propagating wave field is expected to focus back onto the source(s) location(s), although the dominant source is, in this specific case, partially masking the smaller one. We have to consider both temporal and spatial retrofocusing on the source(s) location(s), which leads to two representations of the results of our TR simulations:

- The temporal focusing analysis is concerned with the signal recorded during the TR backward propagation at the original forward propagation source(s) location(s). The reconstruction of the waveform of the originally injected signal (see, e.g. figure 2(a) reported in the next subsection) indicates temporal focusing. This is sufficient for the reconstruction of an unknown source(s), but is not related to imaging the source(s) location(s).
- The spatial focusing analysis deals with a map of the maximum in time of the local displacement (or strain field or elastic energy). It is calculated to localize the region in which the displacement reaches higher values than those in other regions of the specimen (see, e.g. figure 3 reported in the next subsection); such focusing is essential for the localization of an unknown source and this representation usually defines the spatial focal spot.

For the latter case, in this paper we consider the map of the maximum of the displacement in time in any position, defined by the function:

$$M(x, y, z) = \max[q(x, y, z; t)]_t, \quad (2)$$

where $q(x, y, z; t)$ is the norm of the displacement in the position (x, y, z) as calculated at time t from a numerical

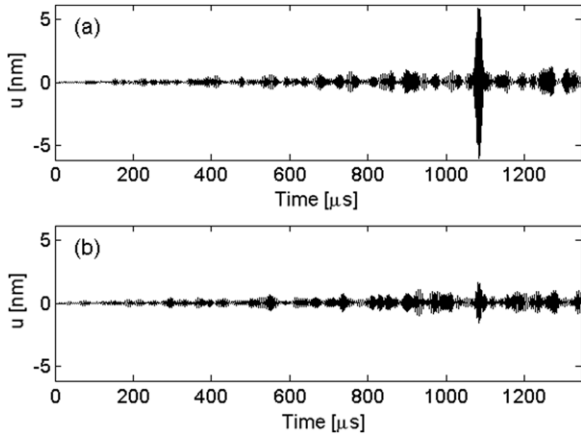


Figure 2. Reconstructed time signals using classical TRA at the location of S_1 (a) and S_2 (b).

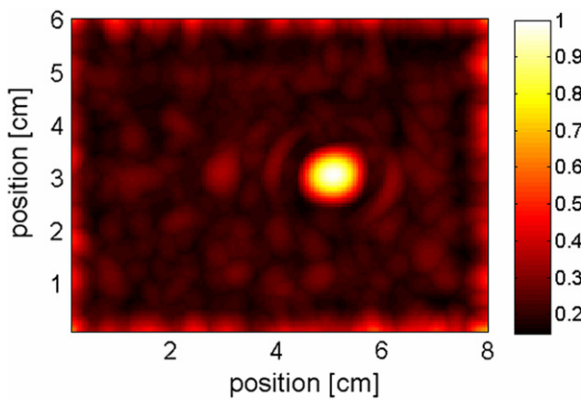


Figure 3. Plot of the maximum displacement recorded on the upper surface of the block, as defined by equation (2). The image indicate good temporal focusing on the stronger source (S_1), while the weaker one is completely masked. (Colour online.)

simulation [12]. In the corresponding experimental case, scanning the surface of the specimen [25] with an out-of-plane laser vibrometer yields only the vertical component of the velocity vector wave field (see section 6).

3.3. Results

In this section, numerical results of the propagation of the time reversed signal $w_k(t)$ are reported to show the focusing resulting from a TR simulation. For this purpose, the signals have been time reversed choosing $t_0 = 0$. Also, a large time window $\Delta = 1.1$ ms is used, to compensate for the small number of receivers by exploiting the information contained in the full signal.

The temporal focusing at the source locations is analysed in figure 2. Here, the signals (in-plane displacements) recorded at the positions of S_1 and S_2 during back propagation are shown versus time. Reconstruction of the larger source is evident (figure 2(a)), with optimal time compression of the signal and excellent reconstruction of its waveform (defined in equation (1)). The time of focusing is the time expected and corresponds to the time window length Δ used for the inversion of the signals. The out-of-plane components of

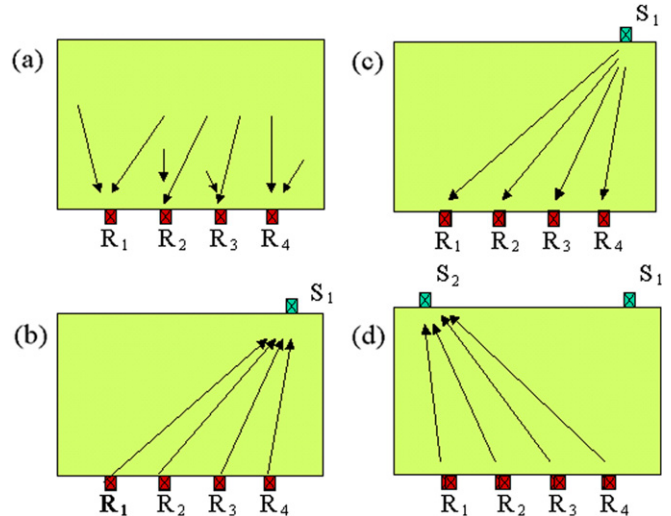


Figure 4. Schematic description of the four steps in the SSR method. See also figure 5 in which examples of signals involved in the different steps are reported.

the displacement are almost negligible (not reported here for brevity), in agreement with the original choice of sources injecting an in-plane displacement. Reconstruction and time compression at S_2 (figure 2(b)) are far less efficient. It is evident that, as shown in section 4, temporal focusing at the smaller source depends on the amplitude of the dominant source and fails if the amplitude of S_1 is too large (e.g. at $A_1 = 10A_2$). The spatial map of the matrix M defined in equation (2) is shown for the upper plane ($z = 0$) in figure 3. Large displacements are concentrated only around S_1 , while there is no evidence of illumination of S_2 . In fact, the spatial focal spot is concentrated around the dominant source only.

4. The SSR method

The example reported in the previous section (together with those that are reported in section 5) indicates failure of the TR procedure for imaging when one of the sources is dominating the other(s). As one may expect, the limiting ratio between the amplitudes of the sources, for a satisfactory localization of the smaller one, depends on several factors related to the experiment performed, but such a limit always exists.

Provided the sources are not too closely spaced, the same example reported before shows that imaging and signal reconstruction are very good for the dominant source. Starting from this consideration, we present a method for eliminating (reducing) the contribution of the larger sources and obtaining focusing and localization on smaller ones.

4.1. The method

The procedure consists of the following protocol, schematically reported in figure 4:

- *Step 1.* Let us assume we start with an experimental system in which some signals $v_k(t)$ are recorded at the receivers ($k = 1 \dots N$): figure 4(a). Number of sources,

locations and shape of the injected signals $u_j(t)$ are the unknowns.

- *Step 2.* Apply the TR procedure, i.e. signals are time reversed and rebroadcast back from the receivers locations (figure 4(b)), either experimentally or numerically³. To record the signal $u_j^{(1)}(t)$, it is necessary to locate a receiver in the position of the dominant source. A preliminary TR experiment/simulation allows one to define the unknown position by examining the spatial focusing. Then, once known where the receiver has to be located, it is possible to repeat the TR experiment/simulation. The signal $u_j^{(1)}(t)$ can then be recorded. Ideal TR focusing corresponds to $u_j^{(1)}(t) = u_j(t)$, i.e. to complete source reconstruction.
- *Step 3.* Rebroadcast the TR of $u_j^{(1)}(t)$, which should correspond approximately to the solution expected when only the dominant source is active, hence providing signals $v_k^{(1)}(t)$ at the N receivers which can be considered as approximate reference signals (figure 4(c)).
- *Step 4.* Considering the original signals $v_k(t)$ as the approximate sum (exact, except for noise contribution, if the material is perfectly linear) of the independent contributions from the sources, we can build a set of signals by subtracting the reference signals $v_k^{(1)}(t)$:

$$w_k(t) = v_k(t) - v_k^{(1)}(t). \quad (3)$$

$w_k(t)$ contains information deriving only from the non-dominant sources, since the contribution of the dominant source is almost cancelled. Of course subtraction of the signals can be performed only after introducing a proper normalization (e.g. both $v_k(t)$ and $v_k^{(1)}(t)$ normalized to one) and a time delay of one of the two signals (to have phase correlation). The latter, which is generally not trivial, is not necessary when the same time window Δ is always adopted when reversing signals. Finally, $w_k(t)$ is time reversed and rebroadcast. Focusing is expected on the second dominant source (see next subsection for results).

The type of receiver to be located at the source position is of course important. Indeed, the receiver should be able to capture the same kind of signal (longitudinal or shear) which was originally emitted. That is also the case for a normal TR experiment: in the comment for figure 2(a) (in plane source), we have already mentioned that a receiver sensitive to out-of-plane components will not be able to detect any temporal focusing. In contrast, receivers used for the temporal inversion (i.e. those on the lower surface of the specimen), can be arbitrarily chosen, provided the time reversed signal is re-injected in the same form as recorded (out of plane or in plane).

Of course, once the first and second dominant sources are localized, one can restart from step 2 locating a receiver in each of the two source locations. In principle, we can repeat the procedure to locate all sources.

³ In the absence of any *a priori* initial information about the sources, the TR rebroadcast is performed via a numerical simulation using an accurate model of the background medium. In the presence of the information that the sources are located on the boundaries of the sample, the backward propagation is performed experimentally in the real medium.

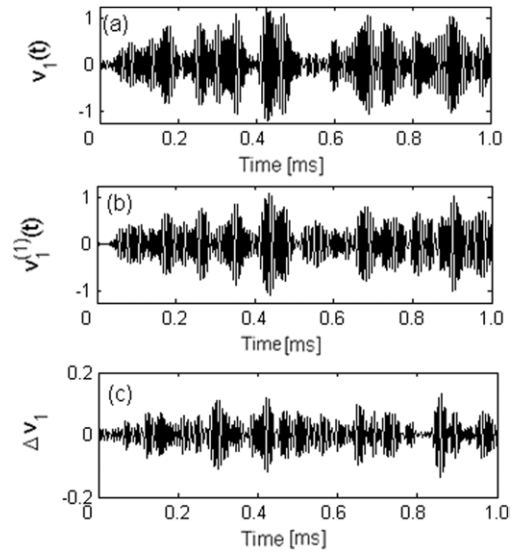


Figure 5. Signals at receiver #1 in the successive steps (see figure 4) of the SSR method. (a) Step 1: the detected signal $v_1(t)$; step 2: the signal re-injected is that reported in figure 2(a); (b) step 3: the detected signal $v_1^{(1)}(t)$. Note the common features with $v_1(t)$; (c) step 4: the subtraction of the two signals give the signal $w_1^{(1)}(t)$ to be re-injected for step 4 of the SSR method. Note the smaller scale of the y-axes in subplot (c).

4.2. Numerical results

Let us now apply the method to the case reported in section 2: $A_1 = 5A_2$. The first two steps of the procedure have been already discussed and the signal re-injected from the location of source 1 (time reversed version of the signal $u_1^{(1)}(t)$) is reported in figure 2(b). In figures 5(a) and (b) we plot a small portion of the time signals $v_1(t)$ and $v_1^{(1)}(t)$ at the receiver #1, after normalization. Their correlation is very good, indicating the validity of the assumption that $v_k^{(1)}(t)$ reconstructs a large part of $v_k(t)$, namely that due to S_1 . The difference $w_1(t)$ of the two signals is reported in figure 5(c).

Implementation of step 4 is then performed. The temporal signals recorded in the position of the two sources are plotted in figures 6(a) and (b) (S_1 and S_2 , respectively), while the matrix M at $z = 0$ is plotted in figure 6(c). A slight improvement in the temporal focusing at S_2 is to be noted, which is more important if we compare it with the reduction of the signal at S_1 , accompanied by a loss of time compression. The side lobes (smaller foci surrounding the main one) are to be expected, if we consider that the TRA procedure (i.e. step 2) reconstructs optimally the central part of the source signal, while its shape is slightly distorted far from the centre. More meaningful is the improvement in spatial focusing, where the weak source begins to be illuminated.

Of course, a lower limit for the ratio A_1/A_2 always exists for the success of this method. This limit depends strongly on the configuration used (size and shape of the specimen, number of transducers used, time window length, etc).

5. Improvements

The results reported in the previous section illustrate the feasibility of source selection with a very simple and direct

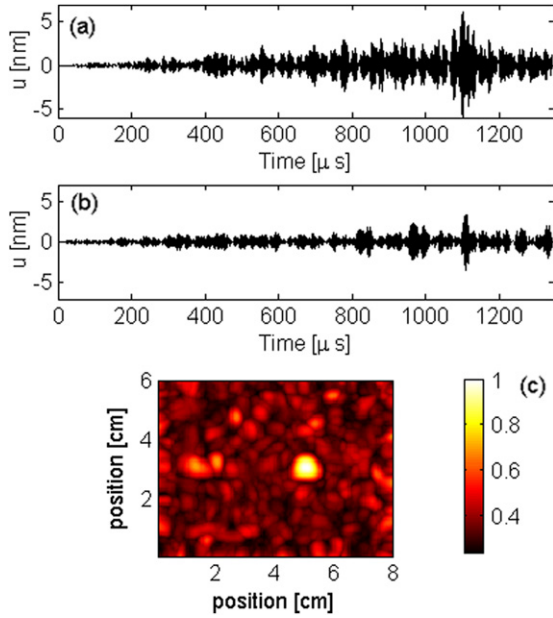


Figure 6. Results of the SSR method for two sources with $A_1 = 5A_2$. (a) Temporal signal at the source S_1 . Compare with figure 2(a); (b) temporal signal at the source S_2 . Compare with figure 2(b); (c) plot of the maximum displacement recorded on the upper surface of the block, as defined from equation (2). Compare with figure 3. Note the improvements in the reconstruction of the time signal at S_2 . (Colour online.)

approach, which can also be implemented in a real experiment. Nevertheless the quality of such results (figure 6) is not entirely satisfactory. A few improvements are possible and are discussed here.

5.1. Windowing of the time reversed signals

The third step of the proposed method consists of the TR of the signals recorded at the position of the dominant source by a properly placed transducer. However, by reversing the full time signal in a window of length Δ , we have not yet fully exploited the information available in that signal. Indeed, we are not using time compression of the signal, i.e. the fact that the original source is reconstructed in a small time window around the focal time. As a consequence, improvements can be expected if only a small portion of $u_j^{(1)}(t)$ is used for inversion in step 3. To accomplish this, we rebroadcast the reversed signal of $u_j^{(1)}(t)$ using the same time window Δ as in the previous section, to avoid problems with the time delays in the subtraction process to be done in step 4. In addition, we force the signal to zero, except in a small time window centred about the focal time ($1.06 \text{ ms} < t < 1.14 \text{ ms}$).

The results after step 4, are reported in figure 7. The improvement of the temporal compression at S_2 is significant and illumination of the lower amplitude source is now evident even though it is smaller in amplitude than the dominant source.

5.2. Iteration of the selection procedure

Iteration of the procedure described in the previous section can be applied to obtain progressive cancellation of the dominant source and/or illumination of other minor sources. At step 4

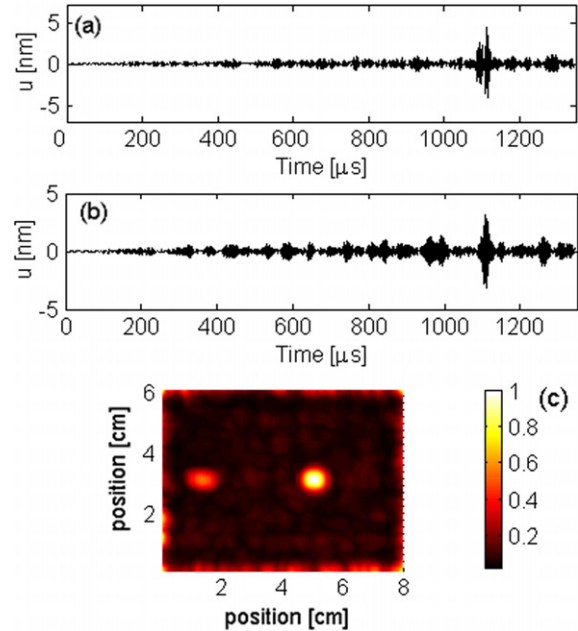


Figure 7. Results of the SSR method for two sources with $A_1 = 5A_2$ after windowing the reversed time signals. (a) Temporal signal at the source S_1 . Compare with figure 6(a); (b) temporal signal at the source S_2 . Compare with figure 6(b); (c) plot of the maximum displacement recorded on the upper surface of the block, as defined from equation (2). Compare with figure 6(c). Note the improvements in the reconstruction of the time signal at S_2 and the appearance of a weak illumination of the S_2 position. (Colour online.)

we record the signal $u_j^{(2)}(t)$ in the position of the dominant source, time reverse (windowing it as discussed in the previous subsection) and re-inject it. Then, we record the signals $v_k^{(2)}(t)$ at the receiver positions and construct a new subtracted signal:

$$v_k^{(3)}(t) = v_k^{(2)}(t) - [v_k(t) - v_k^{(1)}(t)]. \quad (4)$$

Finally, we time reverse and rebroadcast it.

To explore the feasibility of the iteration we have considered a different ratio of the original input amplitudes: $A_1 = 10A_2$. In figure 8 we report the temporal signals in the source's positions and the plot of the matrix M as resulting from a usual TR procedure. As expected, the weak source is not illuminated and no temporal compression is visible at the position of the weaker source. The first iteration of the selection procedure (figure 9) indicates partial reconstruction of the weak signal and partial illumination of the lower amplitude source, but still S_1 is by far the dominant one. Finally, after iteration of the procedure we observe that only the weaker source is illuminated and temporal compression at S_1 is very poor (figure 10).

6. Experimental validation

The SSR-TRA procedure is formally straightforward and easy to implement. From a theoretical point of view, we have shown that the method works even if the signal at the dominant source is not perfectly reconstructed, e.g. due to the use of a finite number of receivers and to the fact that the point of the dominant source does not behave as a sink. Nevertheless, from

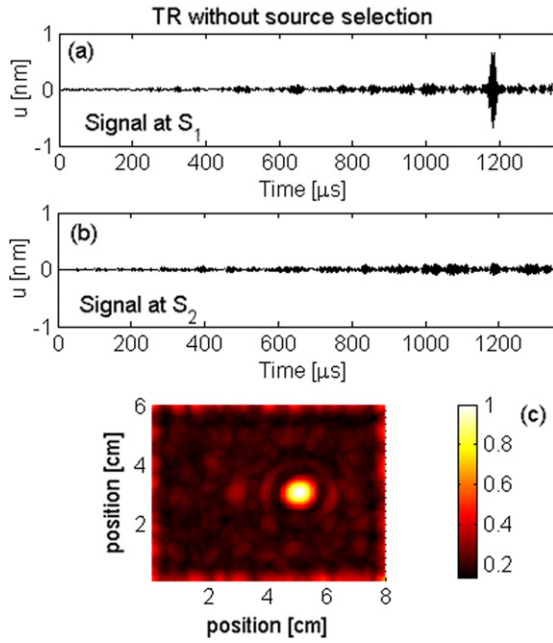


Figure 8. Results of TR without the SSR method for two sources with $A_1 = 10A_2$. (a) Temporal signal at the source S_1 ; (b) temporal signal at the source S_2 ; (c) plot of the maximum displacement recorded on the upper surface of the block, as defined from equation (2). (Colour online.)

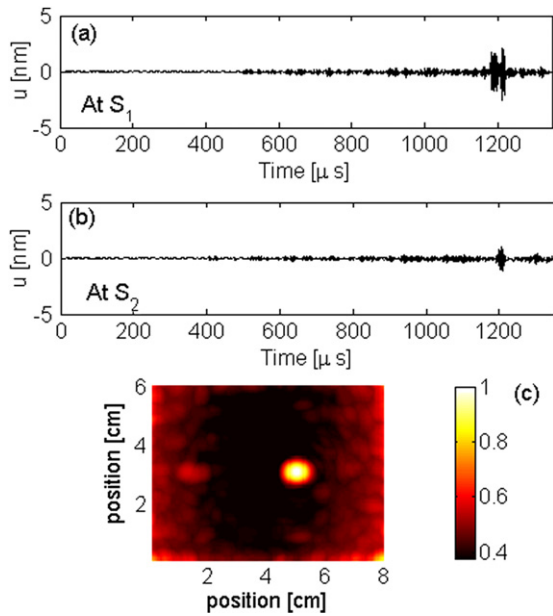


Figure 9. Results of the SSR method for two sources with $A_1 = 10A_2$ after windowing the reversed time signals. (a) Temporal signal at the source S_1 . Compare with figure 8(a); (b) temporal signal at the source S_2 . Compare with figure 8(b); (c) plot of the maximum displacement recorded on the upper surface of the block, as defined from equation (2). Compare with figure 8(c). Note the improvement in the reconstruction of the time signal at S_2 and the appearance of a very weak illumination of the S_2 position. (Colour online.)

an experimental point of view, additional complications may affect the success of the method:

- Limitations are due to the finite size of the transducers (sometimes larger than that of the focal spot), which

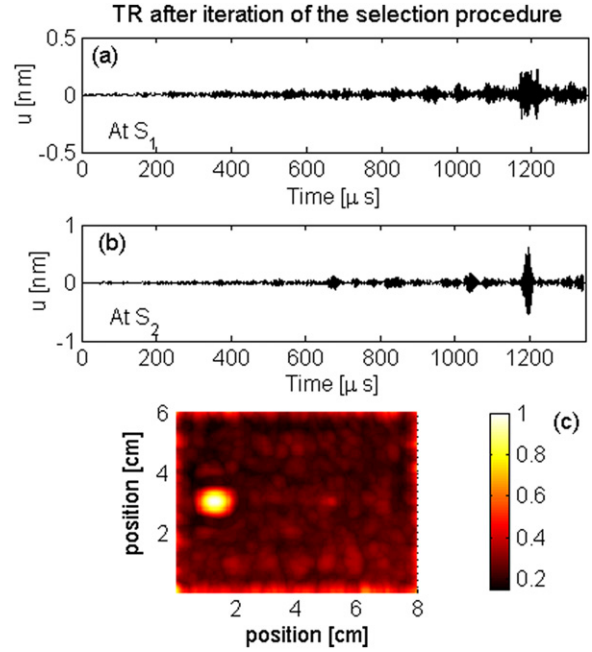


Figure 10. Results after one iteration of the SSR method for two sources with $A_1 = 10A_2$ after windowing the reversed time signals. (a) Temporal signal at the source S_1 . Compare with figure 9(a); (b) temporal signal at the source S_2 . Compare with figure 9(b); (c) plot of the maximum displacement recorded on the upper surface of the block, as defined from equation (2). Compare with figure 9(c). Note the improvement in the reconstruction of the time signal at S_2 and the complete cancellation of S_1 with consequent full illumination of S_2 . (Colour online.)

cannot be point-like as in simulations. Further experimental studies [41] indicate this limitation to be negligible. Also, the robustness of the TRA procedure with respect to the transducers size has been demonstrated by some of the authors [21].

- The focus is modified by the transducers' narrow-band response and is therefore not a perfect reconstruction of the original source function. The transducers bonded to the sample have the effect of broadening the time signal.
- The signal-to-noise ratio may be very poor, especially if small transducers are used. In addition the use of a laser vibrometer imposes additional noise floor issues.

In this section, we show that, despite such technical problems, the SSR-TRA procedure works well, even using a single TR channel [25,42]. Better results can of course be obtained using a larger number of channels, but are not reported here for brevity.

6.1. Experimental setup

Experiments are conducted employing the use of 'virtual' sources. A virtual source is created by sending energy from a transducer into the sample. A laser vibrometer detects the vibration velocity at a user-defined point, corresponding to the position of the virtual source. The signal detected by the laser is time reversed and re-injected by the transducer, which then creates a time reversed focus at the laser's position (virtual source) [28]. This technique relies on the principle of spatial

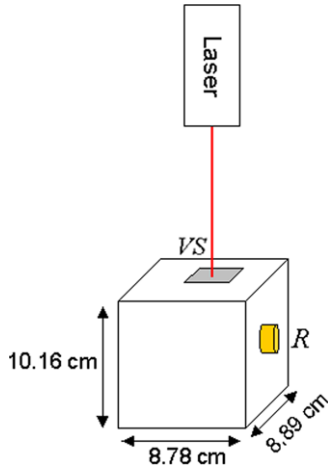


Figure 11. Schematic drawing of the doped glass block sample. S and R represent sources and receivers, respectively. (Colour online.)

reciprocity, i.e. the fact that the signal measured at location B due to a source emission from location A is the same result as the signal measured at location A due to the same source emission from location B [43].

For our experiment, we used a doped glass block measuring $10.16 \times 8.89 \times 8.78 \text{ cm}^3$, with compressional wave speed 4500 m s^{-1} and shear wave speed 2100 m s^{-1} . A diagram of the sample may be found in figure 11. The sample had one 3 mm diameter and 2 mm thick PZT-5 transducer bonded to one side of the block. The input signals used in the doped glass block are of the form:

$$u(t) = A \sin^2\left(\frac{\pi}{\Delta\tau}t\right) \sin(2\pi ft), \quad (5)$$

where A is the amplitude, $\Delta\tau = 50 \mu\text{s}$ is the pulse width, t is time and $f = 200 \text{ kHz}$ is the sine wave frequency.

A laser vibrometer was aimed at the top surface of the glass block as shown in figure 11. Using a laser to create virtual sources, one can locate two sources anywhere on the sample surface. The procedure to create two virtual sources is the following: the transducer generates a signal at amplitude A_1 which is recorded by the laser pointing in a position x_1 , the transducer generates a second signal at amplitude A_2 , which is recorded by the laser pointing in a different position x_2 . The two signals are summed to obtain the signal $v(t)$ corresponding to the ‘virtual’ signal recorded at the transducer as if the two ‘virtual’ sources were active in x_1 and x_2 . This approach works well since the material is linear in the range of amplitudes used here.

The experimental data taken in this paper utilized a sampling frequency of 10 MHz and signal lengths of 32 768 points or about 3.28 ms. The time of focus was set to be about the centre of the 3.28 ms time window, giving 1.64 ms of available data time to collect the direct signal and coda.

6.2. Implementation of SSR-TRA

In the experimental verification of SSR-TRA, we use a single transducer plus a laser vibrometer. The SSR-TRA procedure, similar to that discussed about the simulations, is implemented

as follows:

- The signal $v(t)$ recorded at the transducer is determined as discussed previously, and assumed to be known independently from its origin, which is the unknown of the problem.
- The transducer reinjects the time reversed signal, as in the usual TR without SSR. The laser scans the surface to determine the position of the focal spots and, in a second phase, it records the output signal $u_1^{(1)}(t)$ in the position x_1 of the dominant source.
- Exploiting reciprocity, $u_1^{(1)}(t)$ is time reversed and re-injected from the transducer. $v^{(1)}(t)$ is recorded again by the laser.
- Finally, the signal $v(t) - v_1^{(1)}(t)$ is built, time reversed and re-injected from the transducer, providing the results of the SSR-TRA method.

6.3. Results

As mentioned, we have considered the case of two virtual sources with amplitudes A_1 and A_2 , respectively. The laser vibrometer, aimed at the top surface, was used to scan an area $2.8 \text{ cm} \times 2.8 \text{ cm}$, with the virtual sources located at (7.5, 7.5) cm and (22.5, 19.0) cm, with respect to the scanned area. We have considered the cases $A_1 = A_2$ and $A_1 = 3A_2$.

The spatial focusing map, defined as the map of the maxima of the signal (out-of-plane velocity) detected by the laser at each point of the scanned surface, is reported in figure 12 for the classical TRA and the SSR-TRA, in the left and right columns, respectively. When the sources have the same amplitude, both are illuminated, as expected. The efficiency of SSR-TRA in eliminating the dominant source (which is assumed to be S_1 when the sources have the same amplitude) is evident and consistent with the results of the simulations reported in the previous section.

The method is also efficient in reconstructing the signal. When the two sources have the same amplitude (figure 13), the classical TRA procedure allows both sources to be reconstructed, with optimal time compression of the signal at the expected focal time. When $A_1 = 3A_2$, only the signal at S_1 is reconstructed (figure 14(a)), while the laser detects a completely unfocused signal at the location of S_2 (figure 14(b)). Reducing the dominating source using SSR-TRA, provides the means to almost cancel the signal in the location of S_1 , even though a minor focusing is still present (figure 14(c)). In addition, focusing and time compression is highly enhanced at the location of the minor source (figure 14(d)). Thus, the experimental results presented here confirm the simulation results presented in the previous section.

7. Conclusions

We have presented a SSR method, which, applied together with time reversal acoustics (SSR-TRA), allows one to progressively reduce the illumination of stronger sources, thereby increasing the illumination of weaker ones. We have described the method, provided demonstration using simulation results and showed that the approach can be

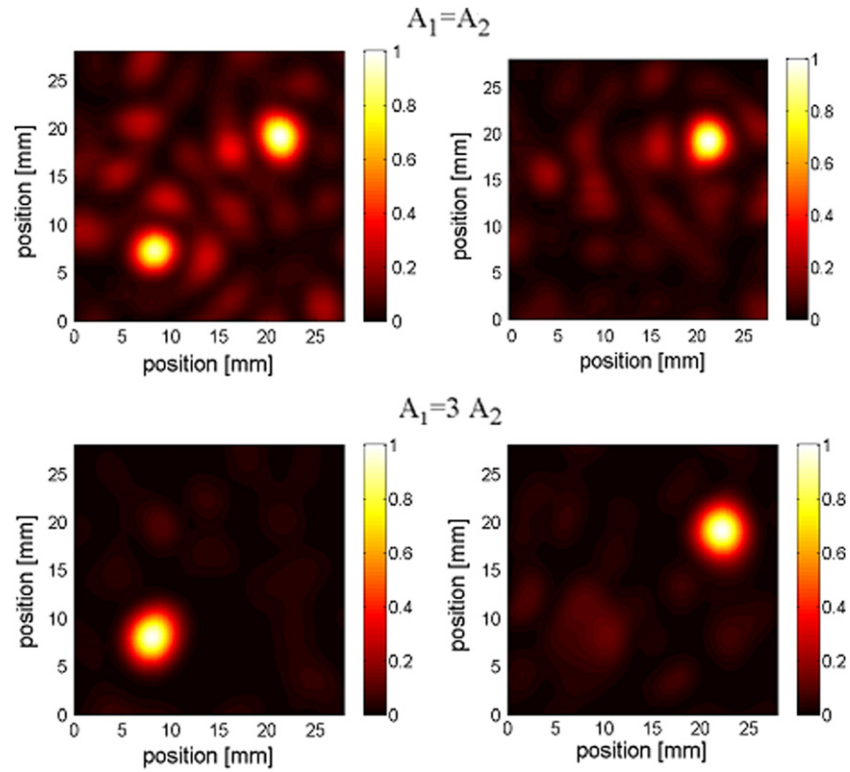


Figure 12. TR focus spatial maps obtained with the usual TRA approach (left column) and after applying the SSR-TRA method (right column) for different ratios of the source amplitudes, as shown in the plot. (Colour online.)

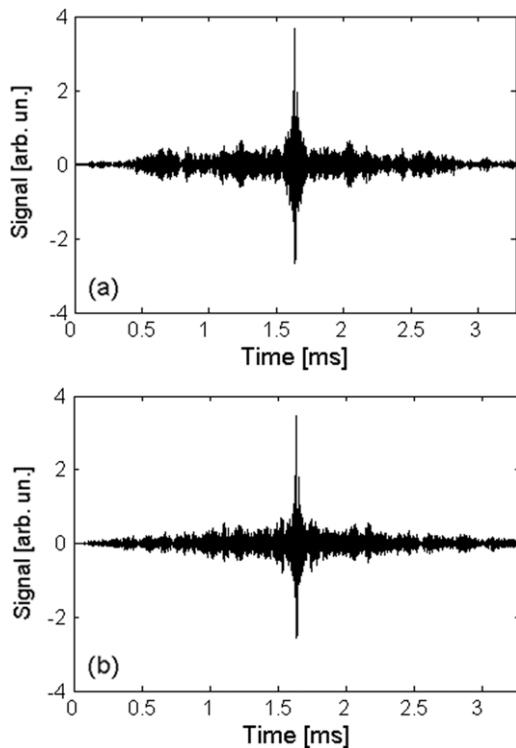


Figure 13. TR focus temporal signals when the sources have the same amplitude: (a) reconstruction at the S_1 ; (b) reconstruction at S_2 . Classical TRA allows optimal reconstruction of both signals, as expected, without any need of the SSR-TRA procedure to be implemented.

implemented experimentally, leading to good results despite using a single TR channel. Indeed, we have shown that the method proposed here is not limited by restrictive assumptions about the configuration of the system.

From an experimental point of view, the SSR method works only to nullify strong surface sources, since a requisite for the procedure is that a receiver must be located on the position of the dominant (to be eliminated) source. Sometimes this is the case, e.g. in the reduction of the nonlinear contribution of a non-perfect transducer, but more often sources/scatterers are embedded in the bulk of the specimen. Nevertheless, in these cases an alternative is possible, by performing the full procedure numerically, after the experimental data of the first forward propagation are given. This would require a detailed material/configuration model.

Furthermore, the waveform of the source signal and the size of the transducers might have an influence, particularly to optimize the procedure. In our opinion, the method may work independently of the kind of source present in the specimen. Indeed, we speculate about the possible application to detection of small nonlinear scatterers, where the waveform of the source signals can be particularly complex. Additional experimental results, not reported here, have also indicated that the method allows one to distinguish sources located only at a distance larger than half the diffraction limit ($\lambda/4$). If this is not the case, modification of the approach have to be figured out.

As already mentioned SSR-TRA is complementary to other approaches developed to obtain selective focusing using TR. In fact, to our knowledge, the existing approaches based

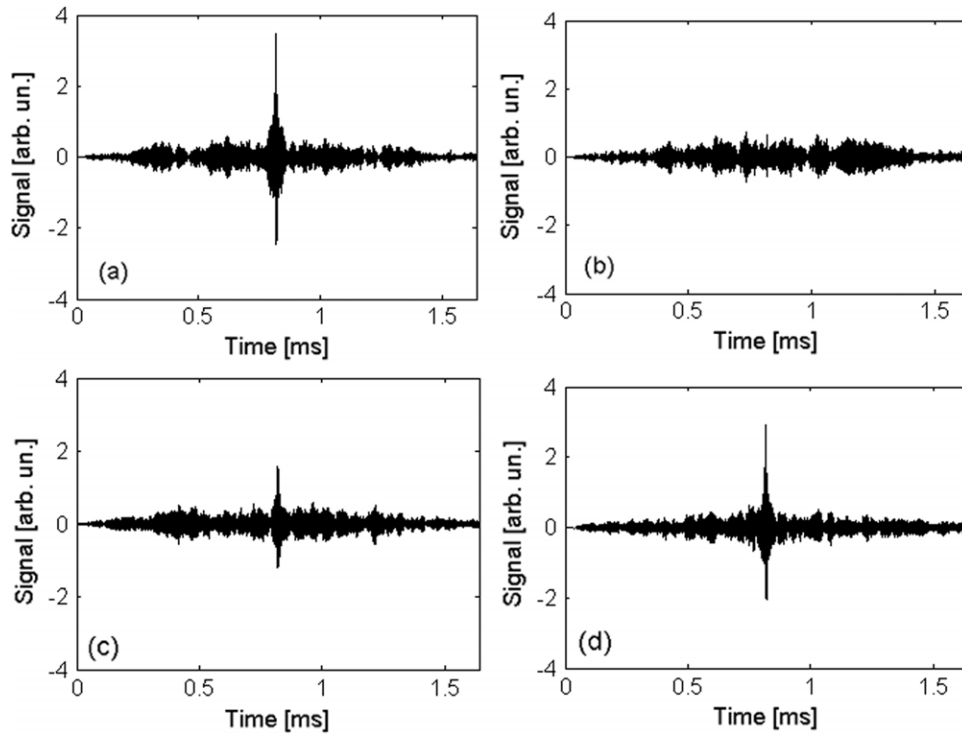


Figure 14. TR focus temporal signals when the sources have amplitudes $A_1 = 3A_2$ demonstrating the SSR method to reduce S_1 and reveal S_2 . The classical TRA approach, provides a near perfect reconstruction of S_1 (a), but not for S_2 (b). Application of SSR-TRA causes a reduction of the focal signal in S_1 (c), and a near optimal focusing at S_2 (d).

on DORT (and its variations) [18–20] address the issue of selectively locating embedded scatterers, but are not applicable to primary source identification. Furthermore, our method, albeit similar in appearance to the reverberation nulling technique developed by Song *et al* [36–38] and to the modified Iterative TR procedure proposed by Montaldo *et al* [39], contains specific features which make SSR-TRA different. In fact, both of these techniques require a large number of TR channels, while, as shown here, SSR-TRA works even with a single transducer. Furthermore, reference signals are always to be analytically calculated (with necessary assumptions and simplifications on the nature of the sources) or determined iteratively, with a complicated and time consuming procedure. In contrast, in SSR-TRA the reference signal is measured with a single step, which furthermore is easier to implement experimentally.

We believe it will be difficult to use SSR-TRA for the identification and localization of weak passive scatterers/targets buried in the medium, in which case other methods [22–26] are more effective. In contrast, the ease of implementation makes our approach useful for applications in the detection of primary sources, including elastic energy releases triggered during earthquake dynamics and/or Acoustic Emission events. In addition, our method may be applied for the detection of nonlinear scatterers in materials (work in progress), since nonlinear scatterers behave as primary sources of higher harmonics, sidebands, etc. In particular, SSR-TRA should enable the reduction of the contributions due to transducers nonlinearity, hence leading to a better illumination of the scatterers.

Acknowledgments

This work has been supported by Institutional Support (LDRD) at the Los Alamos National Laboratory and by the European Community through the project AERONEWS.

References

- [1] Larmat C *et al* 2006 Time-reversal imaging of seismic sources and application to the great Sumatra earthquake *Geophys. Res. Lett.* **33** L19312
- [2] Pluta M, Every A G, Grill W and Kim T J 2003 Fourier inversion of acoustic wave fields in anisotropic solids *Phys. Rev. B* **67** 094117
- [3] Li X, Xu Y and He B 2006 Magnetoacoustic tomography with magnetic induction for imaging electrical impedance of biological tissue *J. Appl. Phys.* **99** 066112
- [4] Fink M, Cassereau D, Derode A, Prada C, Roux P, Tanter M, Thomas J L and Wu F 2000 Time-reversed acoustics *Rep. Prog. Phys.* **63** 1933–95
- [5] Fink M 1993 Time-reversal mirrors *J. Phys. D: Appl. Phys.* **26** 1333–50
- [6] Fink M 1992 Time reversal of ultrasonic fields: part I *IEEE Trans. Ultrason. Ferroelectr. Freq. Control* **39** 555–66
Fink M 1992 Time reversal of ultrasonic fields: part II *IEEE Trans. Ultrason. Ferroelectr. Freq. Control* **39** 567–78
Fink M 1992 Time reversal of ultrasonic fields: part III *IEEE Trans. Ultrason. Ferroelectr. Freq. Control* **39** 579–92
- [7] Fink M 1997 Time reversed acoustics *Phys. Today* **50** 34–40
Anderson B E, Griffa M, Larmat C, Ulrich T J and Johnson P A 2008 Time reversal *Acoust. Today* **4** 5–16
- [8] Montaldo G, Palacio D, Tanter M and Fink M 2000 Building three-dimensional images using a time-reversal chaotic cavity *IEEE Trans. Ultrason. Ferroelectr. Freq. Control* **52** 1489–97

- [9] Borcea L, Papanicolaou G, Tsogka C and Berryman J 2002 Imaging and time reversal in random media *Inverse Problems* **18** 1247–79
- [10] Prada C, Kerbrat E, Cassereau D and Fink M 2002 Time reversal techniques in ultrasonic nondestructive testing of scattering media *Inverse Problems* **18** 1761–73
- [11] Chun H W, Rose J T and Chang F-K 2004 A synthetic time-reversal imaging method for structural health monitoring *Smart Mater. Struct.* **13** 415–23
- [12] Gliozzi A S, Griffa M and Scalerandi M 2006 Efficiency of time reversed acoustics for nonlinear damage detection in solids *J. Acoust. Soc. Am.* **120** 2506–17
- [13] Park H W, Sohn H, Law K H and Farrar C R 2007 Time reversal active sensing for health monitoring of a composite plate *J. Sound Vib.* **302** 5066
- [14] Roux P, Roman B and Fink M 1998 Time-reversal in an ultrasonic waveguide *Appl. Phys. Lett.* **70** 1811–3
- [15] Ulrich T J, Johnson P A and Guyer R 2007 Investigating interaction dynamics of elastic waves with a complex nonlinear scatterer applying the time reversal mirror *Phys. Rev. Lett.* **98** 10430
- [16] Goursolle T, Calle S, Dos Santos S and Bou Matar O 2007 A two-dimensional pseudospectral model for time reversal and nonlinear elastic wave spectroscopy *J. Acoust. Soc. Am.* **122** 3220–9
- [17] Prada C, Fink M and Wu F 1991 The iterative time reversal mirror: a solution to self-focusing in the pulse-echo mode *J. Acoust. Soc. Am.* **90** 1119–29
- [18] Prada C 2002 Detection and imaging in complex media with the DORT method *Imaging of Complex Media with Acoustic and Seismic Waves* ed M Fink *et al* (Berlin: Springer) pp 107–33
- [19] Prada C *et al* 1996 Decomposition of the time reversal operator: detection and selective focusing on two scatterers *J. Acoust. Soc. Am.* **99** 2067–77
- [20] Lehman S and Devaney A J 2003 Transmission-mode time reversal super-resolution imaging *J. Acoust. Soc. Am.* **113** 2742–53
- [21] Griffa M, Anderson B E, Guyer R A, Ulrich T J and Johnson P A 2008 Investigation of the robustness of time reversal acoustics in solid media through the reconstruction of temporally symmetric sources *J. Phys. D: Appl. Phys.* **41**
- [22] Schechter R S, Chaskelis H H, Mignogna R B and Delsanto P P 1994 Real-time parallel and visualization of ultrasonic pulses in solids *Science* **265** 1188–92
- [23] Delsanto P P and Scalerandi M 1998 A spring model for the simulation of wave propagation across imperfect interfaces *J. Acoust. Soc. Am.* **104** 2584–91
- [24] Derode A, Roux P and Fink M 1995 Robust acoustic time reversal with high-order multiple scattering *Phys. Rev. Lett.* **75** 4206–10
- [25] Ulrich T J, Johnson P A and Sutin A 2006 Imaging nonlinear scatterers applying the time reversal mirror *J. Acoust. Soc. Am.* **119** 1514–8
- [26] Draeger G, Cassereau D and Fink M 1997 Theory of the time-reversal process in solids *J. Acoust. Soc. Am.* **102** 1289–95
- [27] Delsanto P P, Johnson P A, Scalerandi M and TenCate J A 2002 LISA simulations of time-reversed acoustic and elastic wave experiments *J. Phys. D: Appl. Phys.* **35** 3145–52
- [28] Sutin A M, TenCate J A and Johnson P A 2004 Single-channel time reversal in elastic solids *J. Acoust. Soc. Am.* **116** 2779–84
- [29] Tanter M, Thomas J-L, Coulouvrat F and Fink M 1999 Time reversal invariance of nonlinear acoustic wave propagation in weakly viscous media *IEEE Ultrason. Symp. (Lake Tahoe, USA)* pp 419–22
- [30] Cunningham K B, Hamilton M F, Brysev A P and Krutyansky L M 2001 Time reversed sound beams of finite amplitude *J. Acoust. Soc. Am.* **109** 2668–74
- [31] Kerbrat E, Prada C, Cassereau D and Fink M 2003 Imaging in the presence of grain noise using the decomposition of the time reversal operator *J. Acoust. Soc. Am.* **113** 1230–40
- [32] Robert J-L, Burcher M and Cohen-Bacrie C 2006 Time reversal operator decomposition with focused transmission and robustness to speckle noise: application to microcalcification detection *J. Acoust. Soc. Am.* **119** 3848–59
- [33] Minonzio J-G, Prada C, Aubry A and Fink M 2006 Multiple scattering between two elastic cylinders and invariants of the time-reversal operator: theory and experiment *J. Acoust. Soc. Am.* **120** 875–83
- [34] Therrien C 1992 *Discrete Random Signals and Statistical Signal Processing* (Englewood Cliffs, NJ: Prentice-Hall)
- Stoica P and Moses R 2005 *Spectral Analysis of Signals* (Upper Saddle River, NJ/Englewood Cliffs, NJ: Pearson Education/Prentice-Hall)
- [35] Gruber F K, Marengo E A and Devaney A J 2004 Time-reversal imaging with multiple signal classification considering multiple scattering between the targets *J. Acoust. Soc. Am.* **115** 3042–7
- [36] Song H C, Kim S, Hodgkiss W S and Kuperman W A 2004 Environmentally adaptive reverberation nulling using a time reversal mirror *J. Acoust. Soc. Am.* **116** 762–8
- [37] Song H C, Hodgkiss W S, Kuperman W A, Roux P, Akal T and Stevenson M 2005 Experimental demonstration of adaptive reverberation nulling using time reversal *J. Acoust. Soc. Am.* **118** 1381–7
- [38] Song H C, Hodgkiss W S, Kuperman W A, Sabra K G, Akal T and Stevenson M 2007 Passive reverberation nulling for target enhancement *J. Acoust. Soc. Am.* **122** 3296–303
- [39] Moura J M F *et al* 2008 Time reversal imaging by adaptive interference cancelling *IEEE Trans. Signal Process.* **56** 233–46
- [40] Montaldo G, Tanter M and Fink M 2004 Revisiting iterative time reversal processing: application to detection of multiple targets *J. Acoust. Soc. Am.* **115** 776–84
- [41] Anderson B E *et al* 2008 Experimental demonstrations of selective source reduction using time reversal acoustics to identify masked sources *J. Phys. D: Appl. Phys.* submitted
- [42] Pautet L *et al* 2005 Target echo enhancement using a single-element time reversal mirror *IEEE J. Ocean. Eng.* **30** 912–20
- [43] Achenbach J D 2003 *Reciprocity in Elastodynamics* (Cambridge: Cambridge University Press)